Figures and figure supplements

Transsaccadic working memory in healthy ageing and neurodegenerative disease

Sijia Zhao and Thomas Parr *et al*.

Figure 1. Location and colour updating across saccades (LOCUS) task. Participants were asked to fixate on a white cross wherever it appeared. They had to remember the colour and location of a sequence of two briefly presented coloured squares (Items 1 and 2), each appearing within a white square frame. They then fixated a colour wheel wherever it appeared on the screen, which served as the target for the second instructed saccade (i.e. a movement from the second fixation cross to the colour wheel location). This cued recall of a specific square (Item 1 or Item 2 labelled within the colour wheel). Participants selected the remembered colour on the colour wheel, which led to a square of that colour appearing on the screen. They then dragged this square to its remembered location on the screen. Saccadic demands were manipulated by varying the locations of the second frame and the colour wheel, resulting in four conditions in their reliance on retinotopic vs. transsaccadic memory: (1) No-Saccade condition providing a baseline measure of within-fixation precision as no eye movements were required. (2) Saccade After Item 1; (3) Saccade After Item 2; (4) Saccades after both items (Two Saccades condition). In all conditions requiring eye movements, saccade vectors were constrained to a minimum amplitude of 8.5° (degrees of visual angle). While the No-Saccade condition isolates retinotopic working memory, conditions (2) to (4) collectively quantify the impact of varying saccadic demands and timings on the maintenance of spatial information, thereby assessing the efficacy of the transsaccadic updating process.

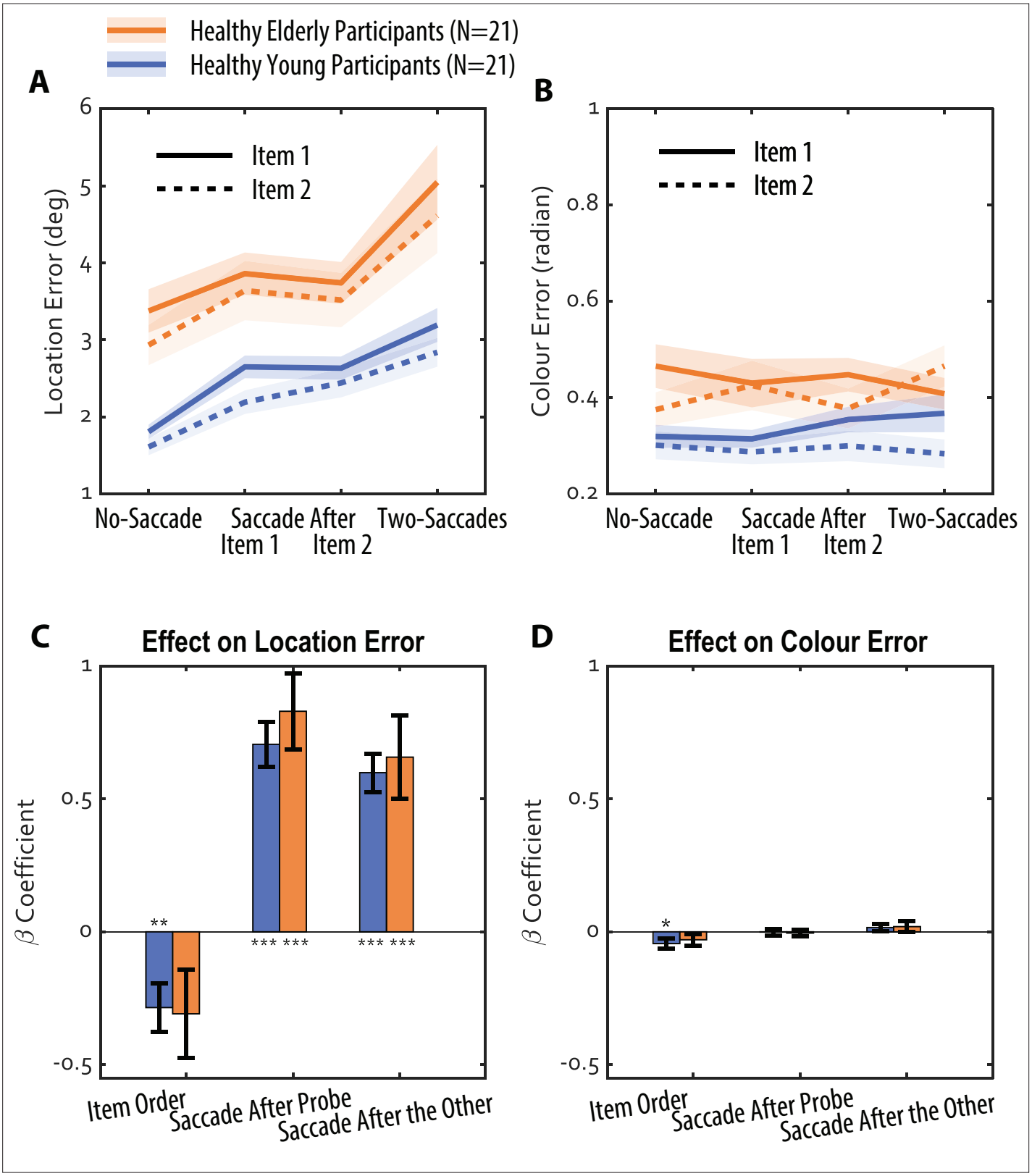

Figure 2. Saccades lead to increased recall error for location but not colour. (**A**) Mean location error for each saccade condition, and for each probed item (Item 1: solid lines; Item 2: dashed lines). Data are shown for young (*N*=21) and elderly (*N*=21) healthy participants. (**B**) Colour error for the same conditions. Shaded error represents ±1 standard error from mean. (**C**) Beta coefficients from a multiple linear regression model predicting location error, illustrating the effect of item order (1 or 2), saccade after the probed item, and saccade after the other item, for young (blue) and elderly (orange)

Figure 2 continued on next page

Figure 2 continued

participants. Error bars represent ± 1 standard errors. (**D**) The same model applied to colour errors, revealing a recency effect but no impact of saccade demands. ** means significantly different from zero p<0.01, *** means significantly different from zero p<0.001.

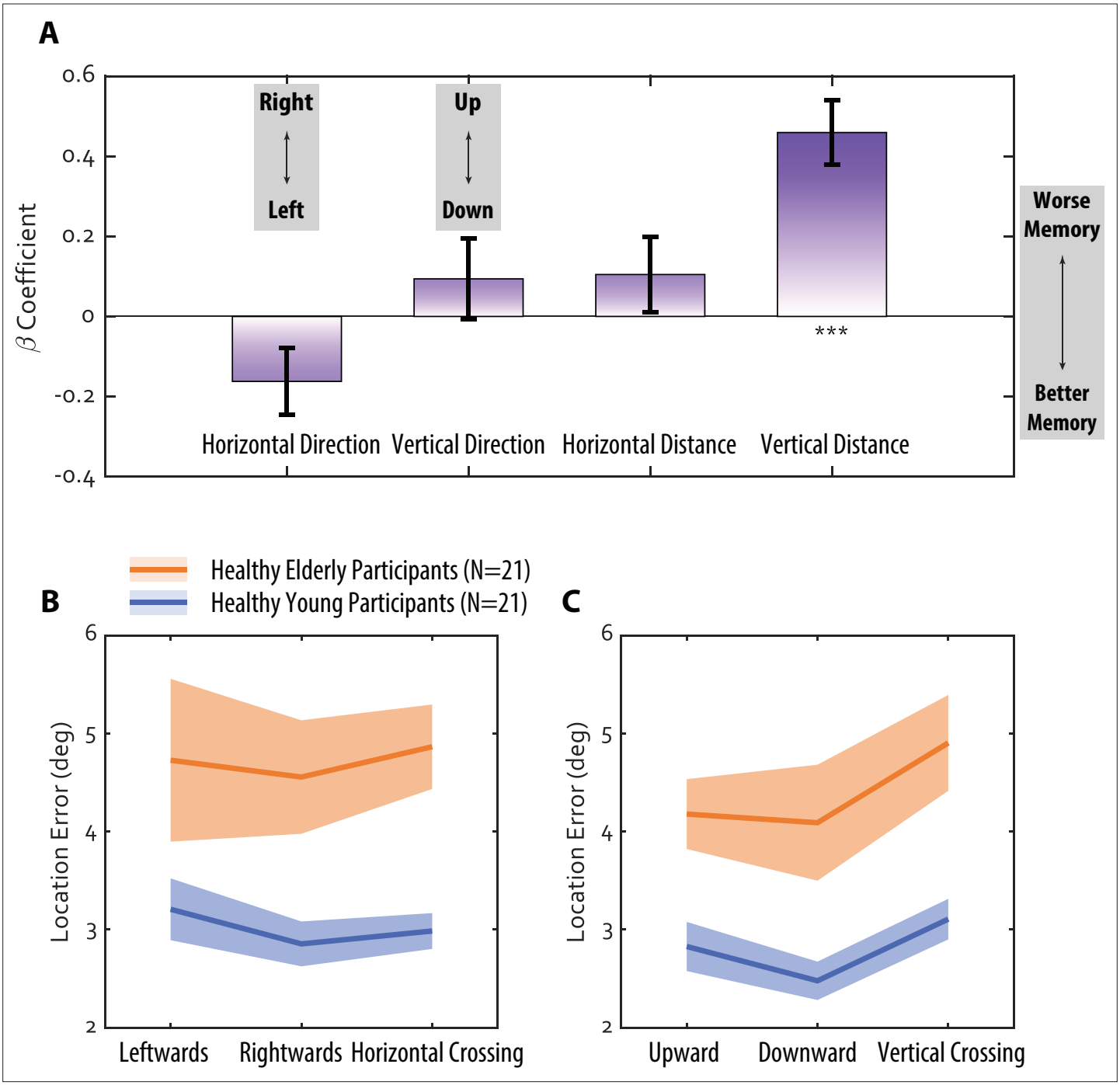

Figure 2—figure supplement 1. Effect of saccade direction and distance on transsaccadic memory. (**A**) Beta coefficients from individual participant models predicting location memory. Asterisks denote significance: **p<0.01, ***p<0.001. (**B**) Breakdown of the two-saccade condition, by horizontal direction and (**C**) vertical direction. Mean location error in the two-saccades condition, categorised by saccade direction: leftwards (consecutive leftward saccades), rightwards (consecutive rightward saccades), horizontal crossing (saccades in opposite directions), as well as upwards (consecutive upward saccades), downwards (consecutive downward saccades), vertical crossing (saccades in opposite directions). No significant differences were observed between conditions within each group.

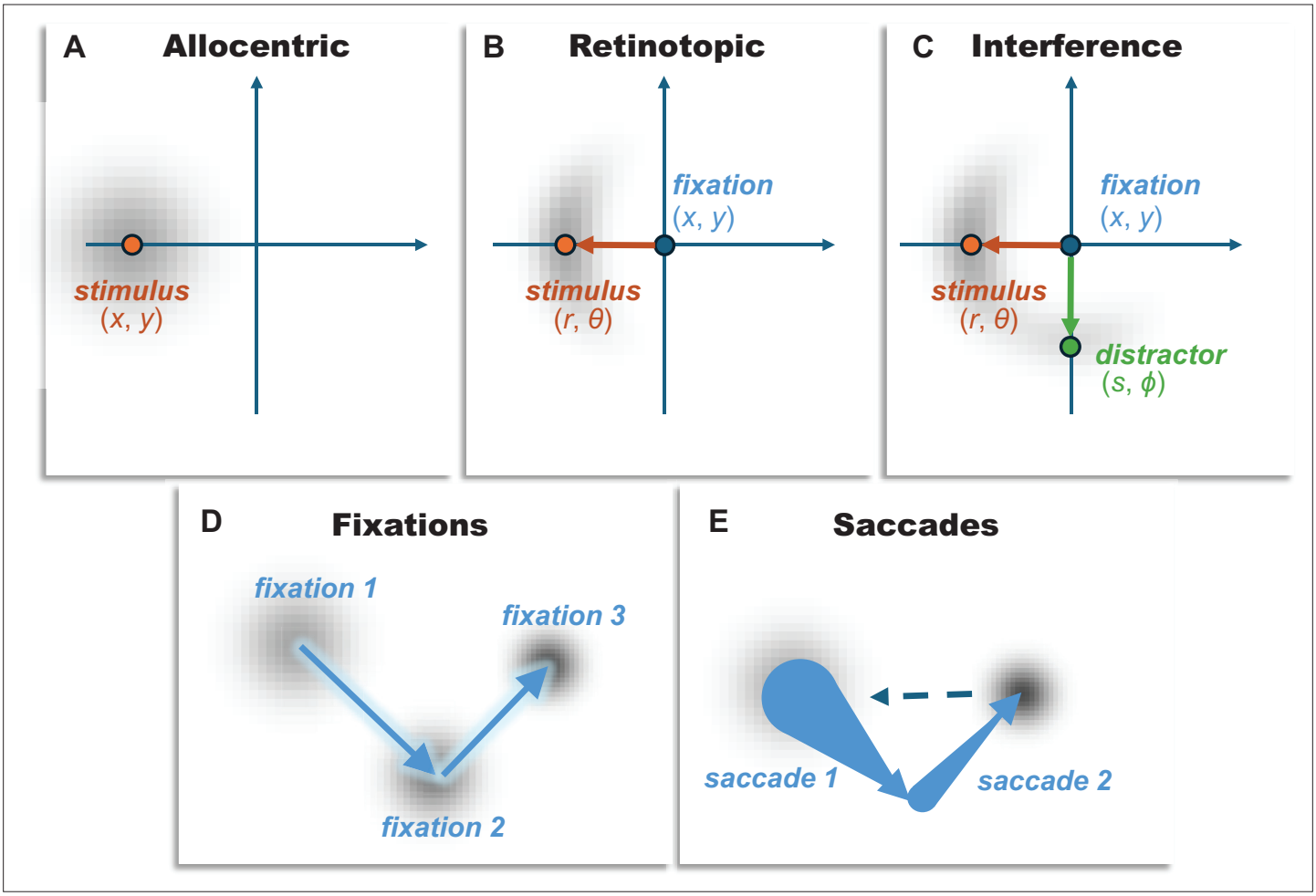

Figure 3. Conceptual illustration of allocentric vs. retinotopic spatial representations. This figure depicts the distinction between various representations of spatial memory. These include allocentric (world-centred) and retinotopic (eye-centred) spatial representation. (**A**) The allocentric panel illustrates a world-centred reference frame, where a stimulus location (*x*,*y*) is represented independently of eye position. The spread of the grey shaded area around the stimulus indicates for this representation the encoding error and subsequent decay since the stimulus was viewed. In this framework, memory error is assumed to increase over time due to a general decay of the stored coordinates, which is treated as a decay in Euclidean space, such that the probability density of a remembered location (coordinates (*x*,*y*)) is a normal distribution whose covariance grows with time centred on the stimulus. This model corresponds to Model 1 in ***Table 1***. (**B**) The retinotopic panel presents an eye-centred reference frame, where the stimulus location is encoded relative to the current fixation point (*x*,*y*) using polar coordinates: radial distance (*r*) and angular direction (*θ*). The orange arrow indicates the vector from fixation to the stimulus, representing these encoded retinotopic coordinates. The grey shaded area here again represents the initial encoding error and subsequent decay, which can be decomposed into radial and angular components. This dual model, incorporating both encoding error and decay in radial and angular components, corresponds to Model 2 in ***Table 1***. It forms the basis for more complex models (Models 3–7 in ***Table 1***) that differentiate between decay of the reference frame itself (e.g. recall of fixation point) and updating based on saccade information. (**C**) The interference panel shows the combination of a stimulus and distractor (translated into the same retinotopic coordinates), with some probability associated with a response to the memory of the distractor stimulus. The lower two panels distinguish between whether the origin of the retinotopic plot is recalled based upon a remembered fixation location (**D**), or whether it is based upon a reconstruction after propagating back through remembered saccade vectors (**E**) —conceptually shown with arrows whose base is large to indicate the (cumulative) uncertainty in the origin points of each vector.

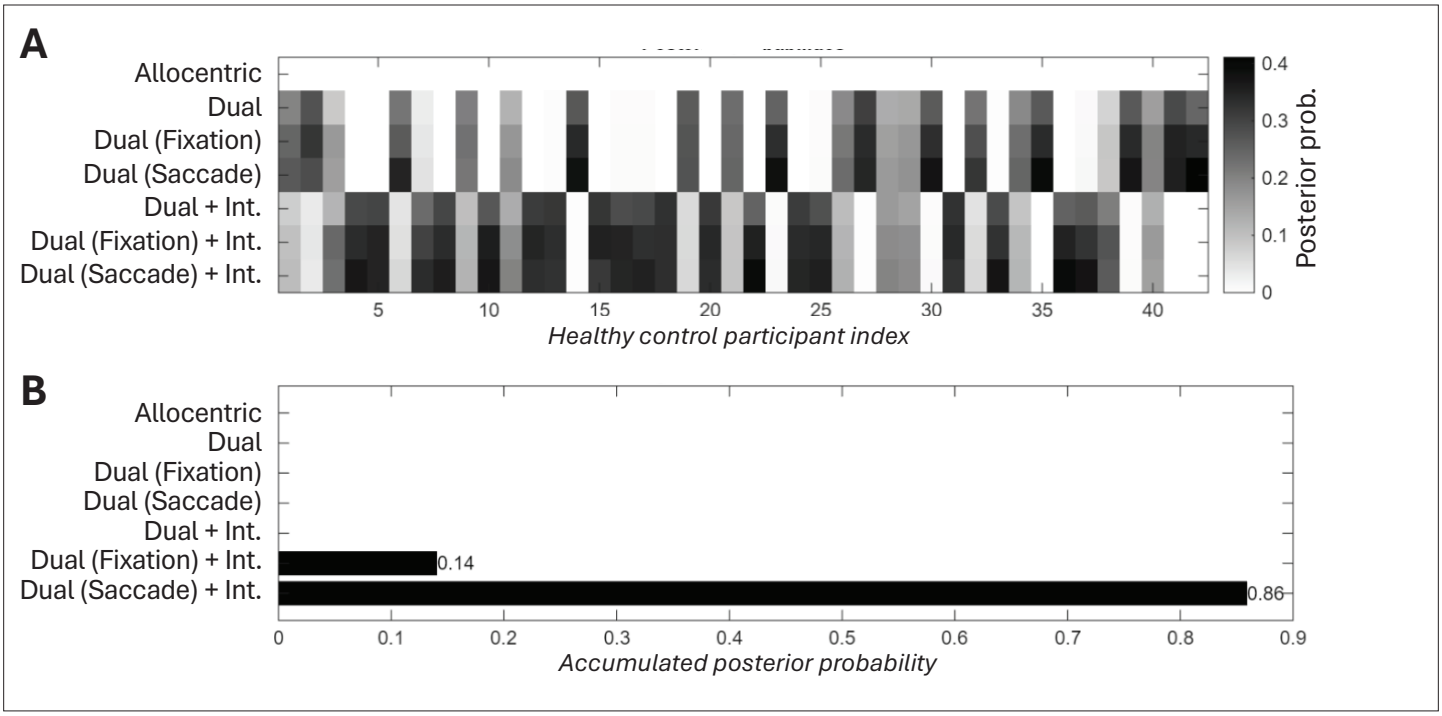

Figure 4. Model comparison results in healthy control (HC) participants (*N*=42). (**A**) Individual participant posterior probabilities. Heatmap illustrates the posterior probability for each of the seven competing models across individual healthy participants. This panel indicates that the 'Dual (Saccade Update)+Interference' model frequently shows the highest posterior probability for individual participants. (**B**) Aggregate model posterior probabilities. Bar chart showing the posterior probability for each competing model, aggregated across all healthy participants.

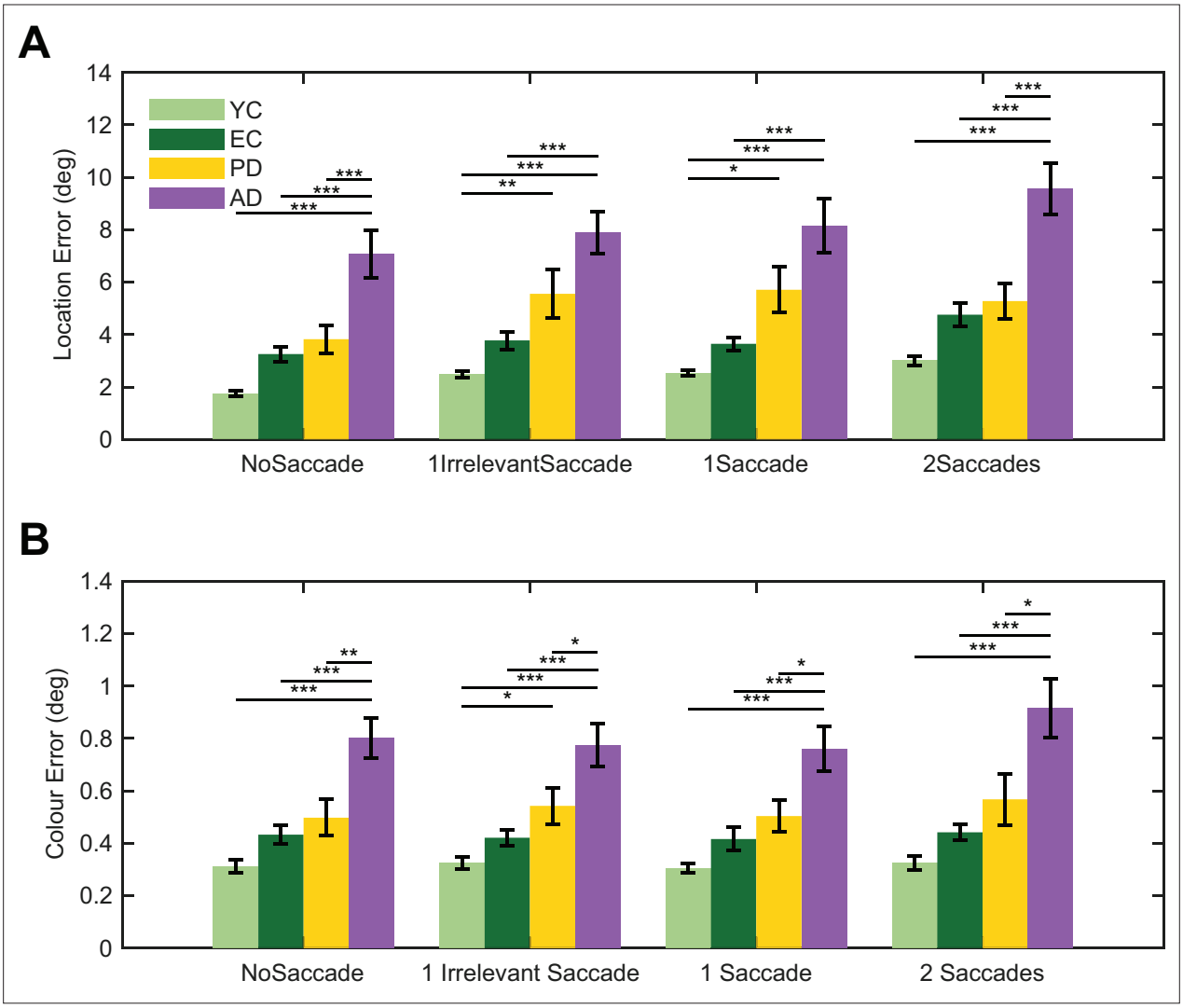

Figure 5. Saccadic interference with spatial memory is preserved across healthy ageing and neurodegenerative conditions, despite group differences in recall error. Saccades lead to increased recall error for location, but not colour, in healthy young (YC, *N* = 21) and elderly (EC, *N* = 21) controls, as well as in patients with Parkinson's disease (PD, *N* = 23) and Alzheimer's disease (AD, *N* = 22). While patient groups exhibit greater overall memory errors, the fundamental pattern of saccadic disruption remains consistent across all cohorts. (**A**) Location error. Mean location error (in degrees of visual angle) for each saccade condition (No-Saccade, 1 Irrelevant Saccade, 1 Saccade, 2 Saccades) for all participant groups. A two-way ANOVA revealed a significant main effect of Group and Condition, but there was no significant Group×Condition interaction ($F(9, 318)=0.46$, $p=0.900$), indicating that the magnitude of saccadic disruption to spatial memory is constant across groups. Post hoc Tukey-Kramer comparisons within each condition between groups confirmed a graded impairment in overall spatial accuracy: AD patients exhibited significantly greater errors than all other groups (e.g. AD vs. YC, EC, PD: all $p<0.001$), PD patients performed worse than both YC and EC (all $p<0.001$), and EC performed worse than YC (all $p<0.001$). The significant post hoc between group comparisons are shown above the bar plots, with Bonferroni multiple comparison correction applied. (**B**) Colour error. Mean colour error (in radians) for each saccade condition across participant groups. For colour memory, a two-way ANOVA revealed a significant main effect of Group but no significant main effect of Condition or Group×Condition interaction. Post hoc comparisons for colour error showed a similar pattern of overall group differences as observed for location memory (all group comparisons $p<0.001$). Error bars represent ± 1 standard error of the mean (SEM). Asterisks denote statistical significance from post hoc comparisons: *: $p<0.05$, **: $p<0.01$; ***: $p<0.001$.

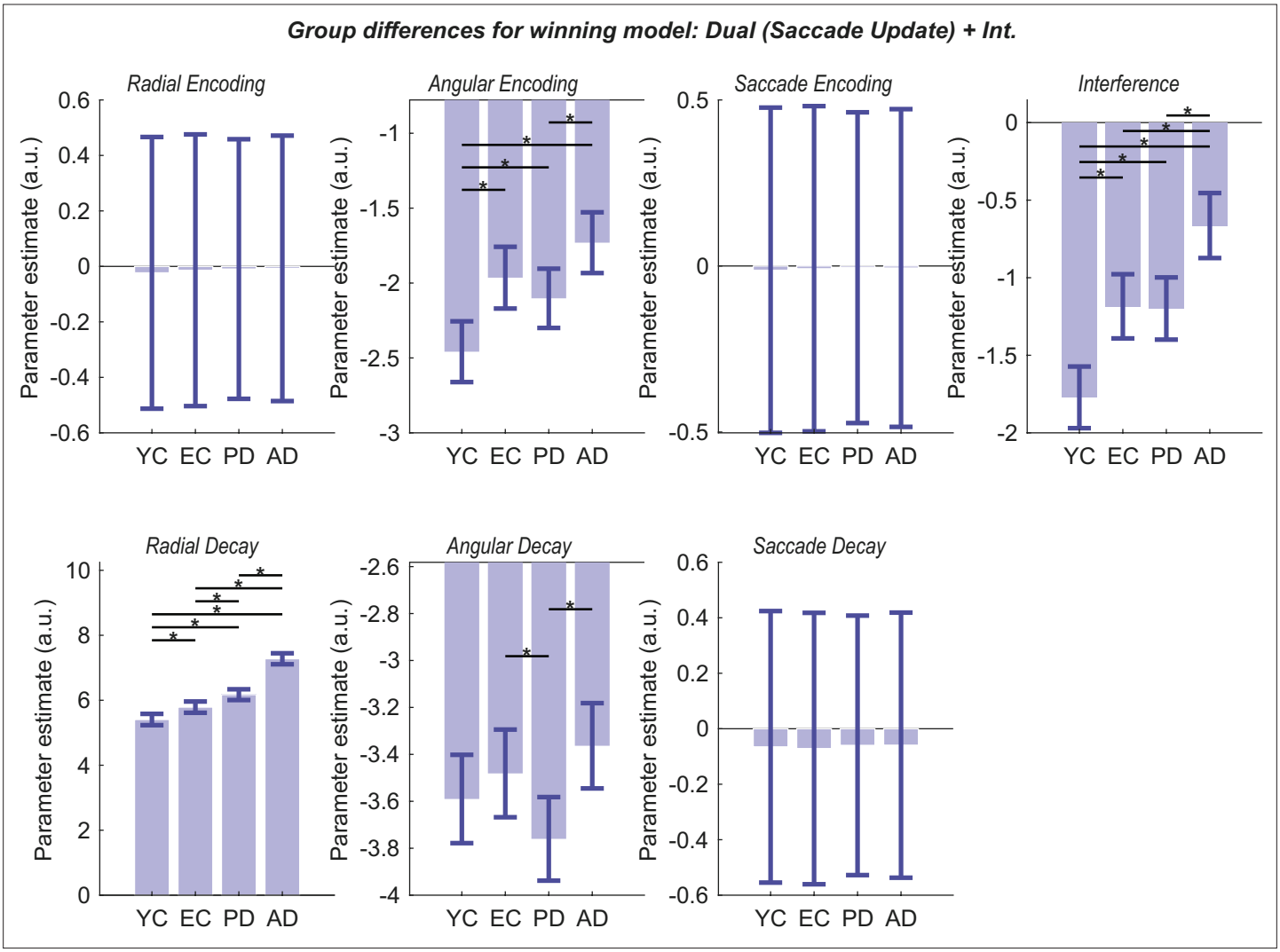

Figure 6. Group differences in winning model parameters. The plots show group-level parameter estimates from the parametric empirical Bayes (PEB) analysis for the winning 'Dual (Saccade)+Interference' model. The y-axis represents the posterior mean of the log-scaled parameter, where a more positive value indicates a greater influence of that parameter on performance (i.e. greater error or faster decay). The exception is the interference parameter, which is effectively a logit parameter, meaning the probability of selecting the distractor is obtained by a sigmoid transform. Error bars represent the 90% posterior confidence intervals. Group differences are indicated by an asterisk (*) if the posterior probability of a difference between the respective parameter estimates is greater than 95%, as calculated from their posterior distributions (i.e. if p(A>B)>0.95 or p(B>A)>0.95). The analysis reveals that Angular Encoding, Angular Decay, Radial Decay, and Interference parameters differentiate the groups. Critically, the EC group shows significant deviations from the YC group in Angular Encoding, Radial Decay, and Interference, providing a model-based profile of healthy age-related spatial memory decline. Notably, parameters related to saccade processing (Saccade Encoding and Saccade Decay) and Radial Encoding do not differ between groups, suggesting that the integrity of transsaccadic remapping is preserved across the lifespan and in early-stage neurodegeneration.

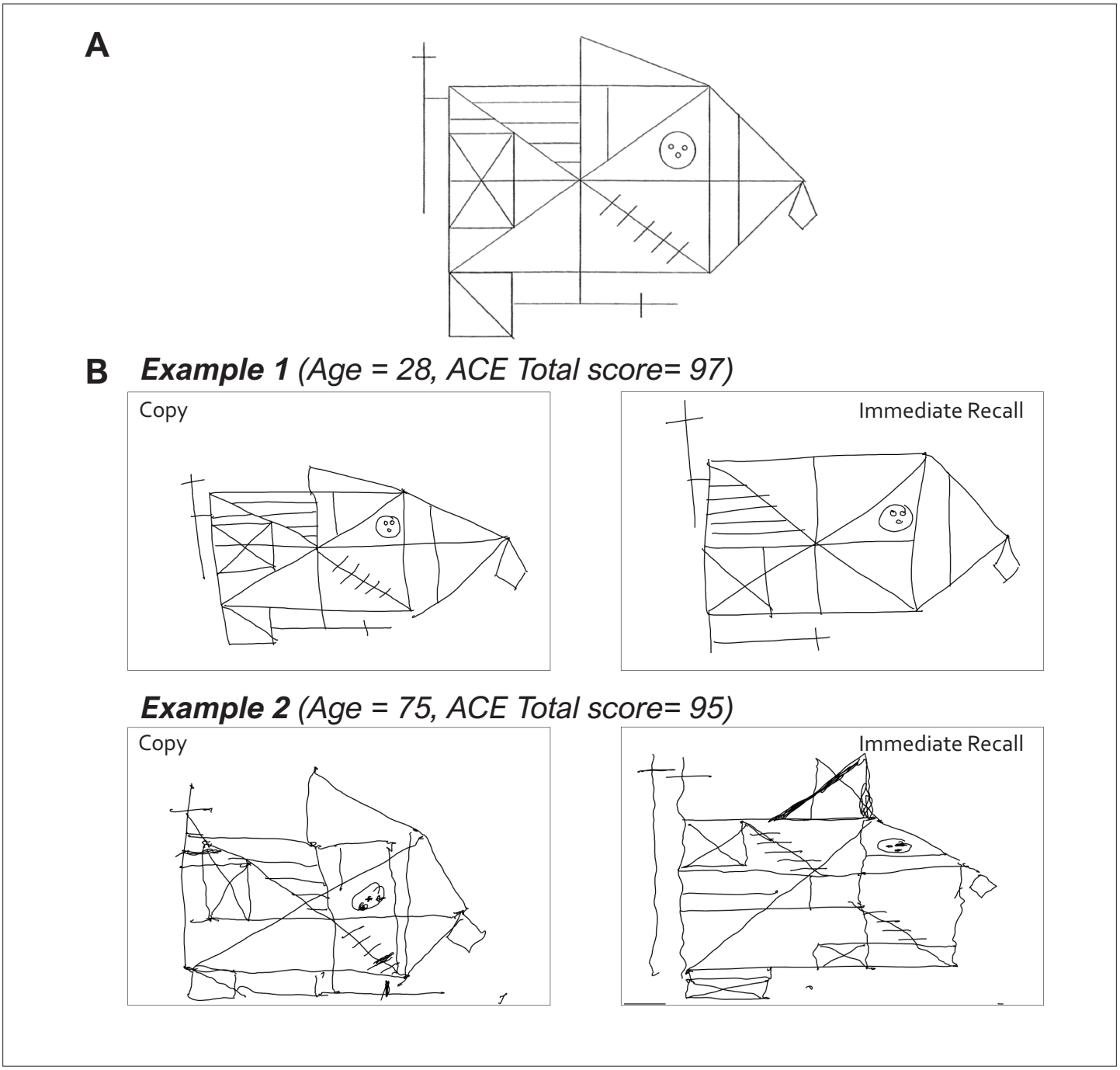

Figure 7. Rey-Osterrieth complex figure (ROCF) copying performance. (**A**) The original figure that participants copied and recalled. (**B**) Examples of ROCF copy and immediate recall tasks from a young and an elderly healthy participant, both with normal cognitive function (ACE total score>88). ACE = Addenbrooke's Cognitive Examination-III.

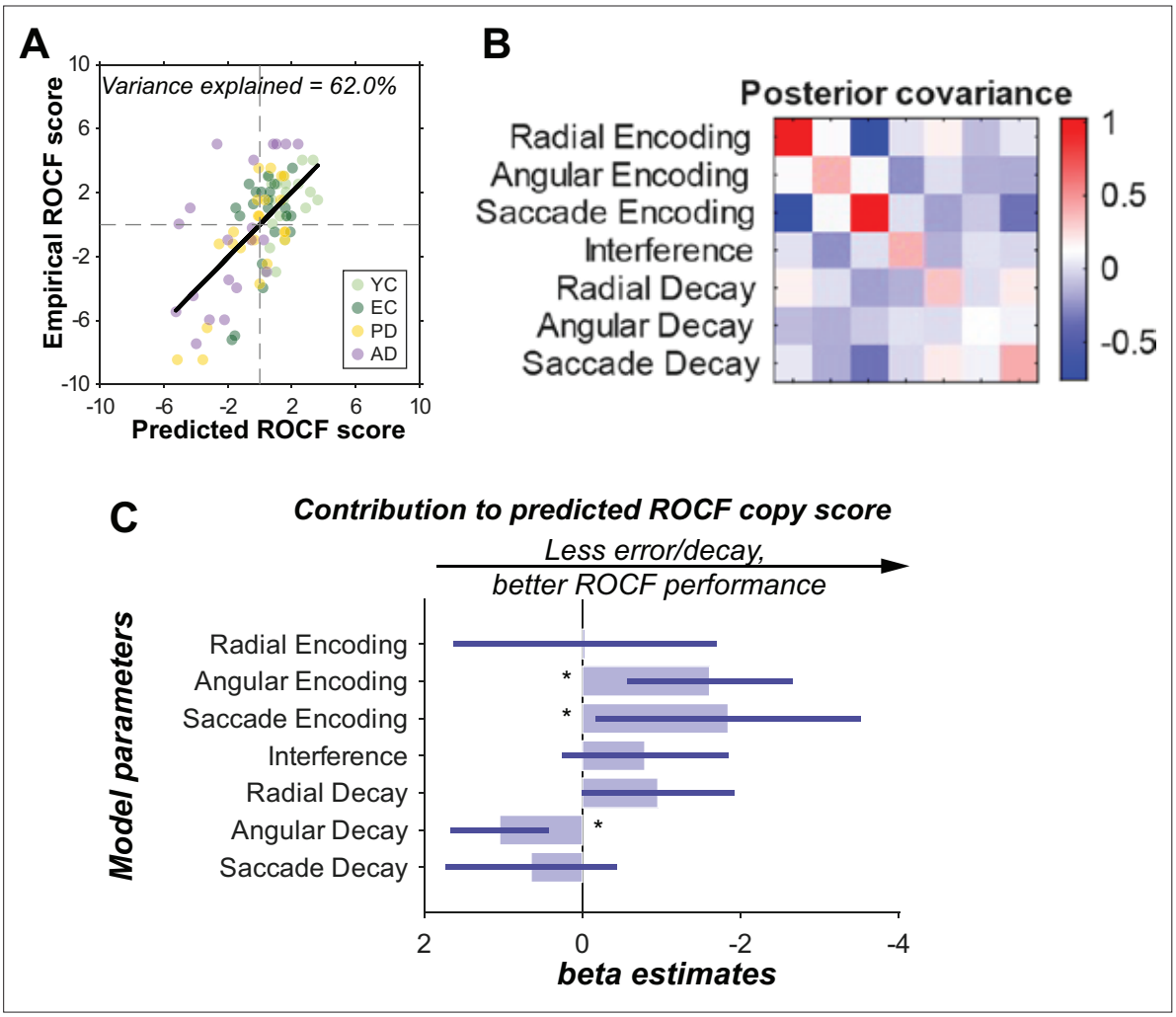

Figure 8. Effect of model parameters on Rey-Osterrieth complex figure (ROCF) copy scores. How model parameters from the winning 'Dual (Saccade)+Interference' model explain variance in ROCF copy performance. (**A**) Predicted vs. empirical scores. A scatter plot of empirical ROCF scores against scores predicted by the fitted linear model. Each point represents an individual participant, coloured by diagnostic group: young controls (YC; light green), elderly controls (EC; dark green), Parkinson's disease (PD; yellow), and Alzheimer's disease (AD; purple). A black line denotes the linear fit across all data. ROCF scores were demeaned across participants. Scores outside of 2 standard deviations from the mean were omitted. The plot title indicates the percentage of variance in ROCF copy scores explained by the model. (**B**) Posterior covariance matrix. A heatmap depicting the posterior covariance between the estimated model parameters (i.e. between the regression coefficients that determine the contribution of each of the parameters from our previous winning model to the ROCF score). Diagonal elements represent individual parameter variances; off-diagonal elements show covariances between parameter pairs. The colour bar provides the scale. (**C**) Estimated parameter contributions. Bar plot displaying the estimated contribution (beta coefficients) of each LOCUS model parameter to the predicted ROCF copy score. Error bars represent 90% credible intervals (1.65 standard deviations of the posterior variance). Asterisks (*) denote parameters whose 90% confidence interval does not encompass zero.

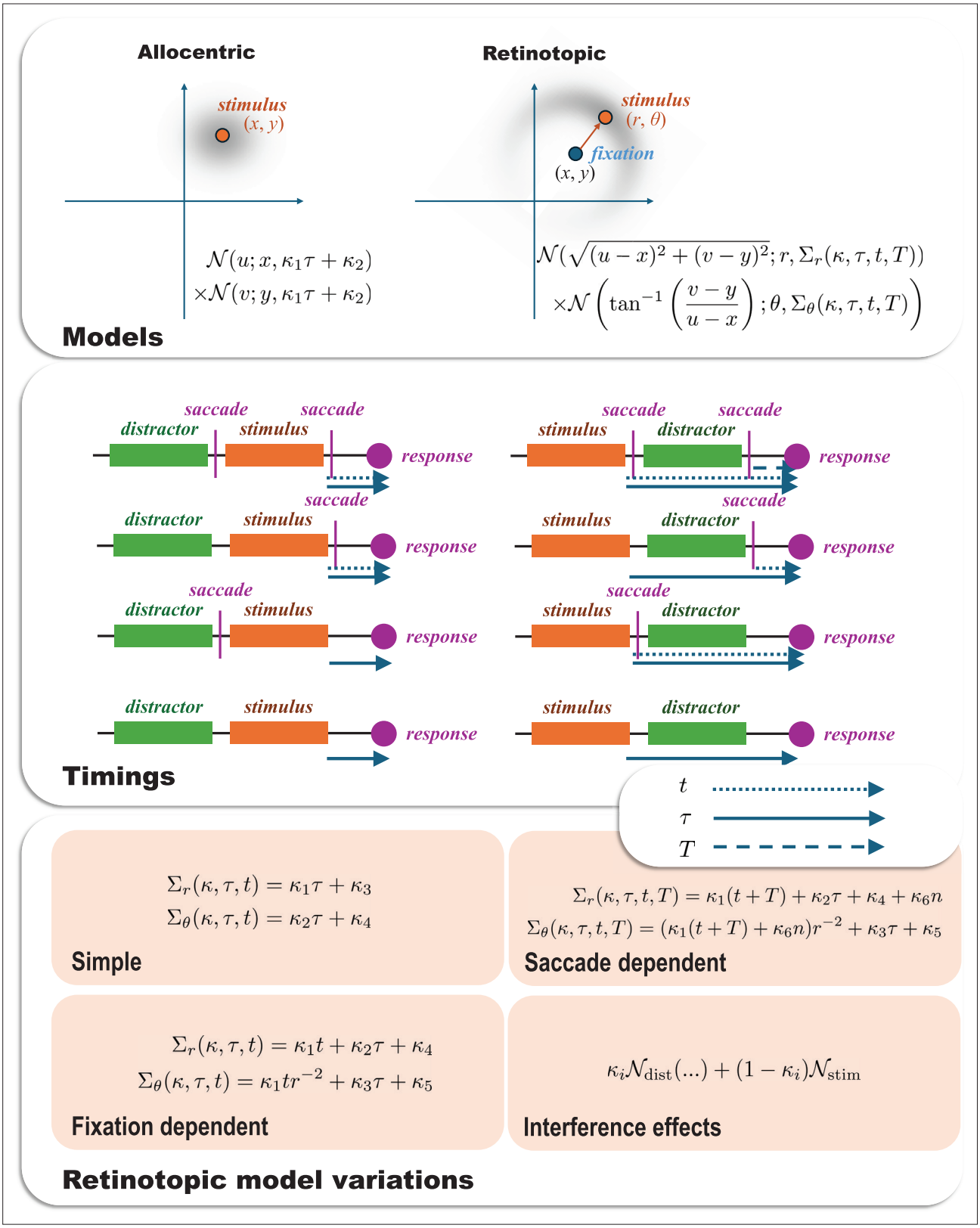

Figure 9. Models and hypotheses. This figure illustrates the form of the models used for our model comparisons. The upper panel shows the distinction between allocentric screen-centred coordinates, which we treat as a decay in Euclidean space, such that the probability density of a response (coordinates (*u*,*v*)) is a normal distribution whose covariance grows with time centred on the stimulus. In contrast, the retinotopic representation uses polar coordinates with both radial and angular decays. There are several ways in which the associated covariance can be formulated, and this depends

Figure 9 continued on next page

Figure 9 continued

upon the different times over which the decay in memory might occur. The different timings in the alternative experimental conditions are shown schematically in the middle panel, dealing with the time since the stimulus was visible (*τ*), the time since the first saccade (if any) since the stimulus was present (*t*), and the time since the second saccade (if any) after the stimulus (*T*). The variations, based on these timings, for the dynamics of the covariance for the retinotopic model, are shown in the lower panel. The simple model assumes that any decay in the fixation location around which the retinotopic coordinates can be captured by decays in the radial and angular coordinates. This implies there is no difference in the form of the decay when the same fixation location is sustained after the stimulus disappears compared to when a subsequent saccade is made. The fixation-dependent model assumes instead that there is an independent decay in the fixation location, which only begins once we have moved our eyes from the location at which we saw the stimulus. In contrast, the saccade-dependent framing assumes that, rather than retaining a memory of fixation location, we reconstruct the fixation location based upon our memory of the saccade vectors made since that fixation. Here, the n variable represents the number of saccades made since the relevant fixation. The interference effects are mediated by computing the distribution we would expect from a response to the target stimulus and the distribution we would expect from a response to the distractor stimulus (translated into the same retinotopic space) and taking a weighted sum of the two.

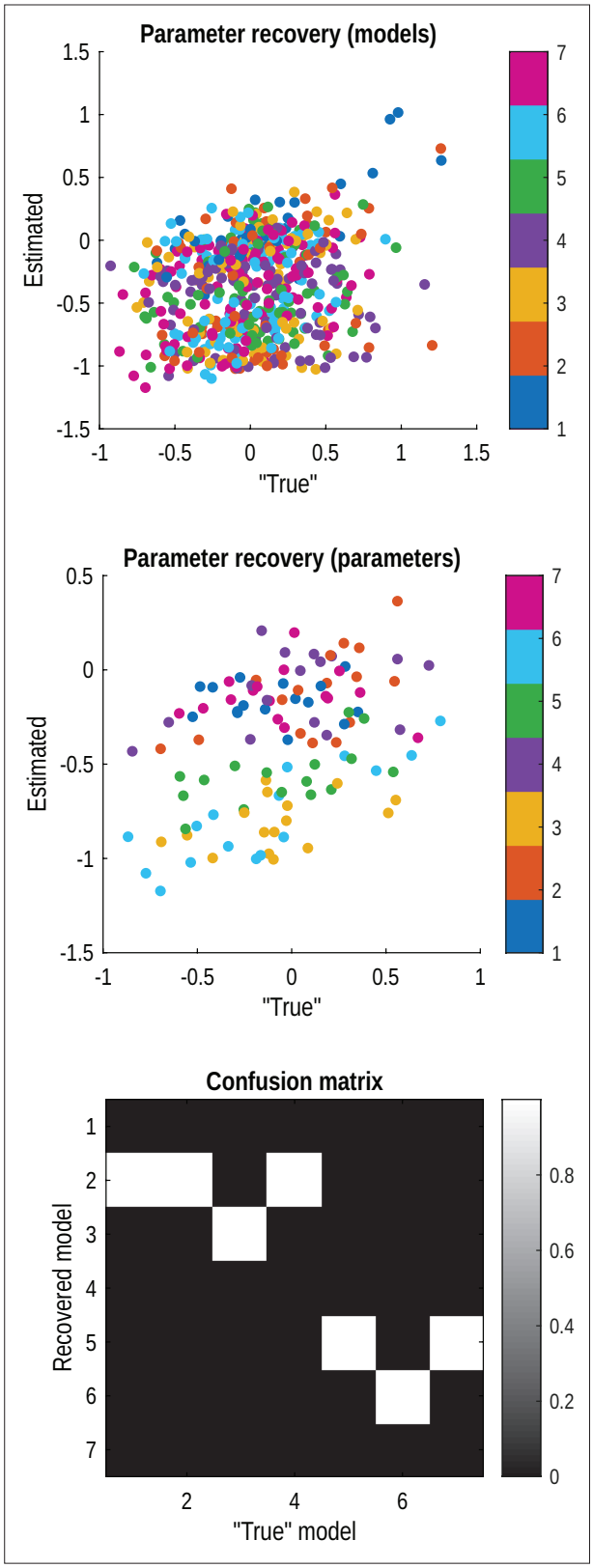

Figure 10. Model recovery analysis. This figure reports the results of a model recovery analysis resulting from simulation of data from each model, for 16 participants each (where a participant is generated by sampling parameters from the model priors). Each participant was fit to all models, and the confusion matrix in the lower panel is computed by accumulating the log marginal likelihoods for each combination of model and synthetic

Figure 10 continued on next page

Figure 10 continued

participant and (softmax) normalising the columns to arrive at posterior probabilities. The upper panel shows all 'true' and estimated parameters recovered when the 'true' models are used on their own datasets. Points are labelled with colours corresponding to the model (see key on the right). Clearly, there is variable veridical recovery across models for the set of sampled parameters. The middle panel presents those estimates for only Model 7 (which in the empirical analysis turns out to be the best explanation). Here, the colours relate to the parameter identities (in the order 'Saccade Decay', 'Radial Decay', 'Angular Decay', 'Radial Encoding', 'Angular Encoding', 'Interference', 'Saccade Encoding'). The correlation coefficients for each of these parameters, respectively, are: –0.62, 0.12, 0.55, 0.35, 0.27, 0.90, 0.17, indicating at least a weak positive correlation for all but the 'Saccade Decay' parameter, and particularly good recovery of the 'Interference' parameter. Of note, those parameters with a weak correlation coefficient do not move far from their (zero) prior expectations, highlighting that those parameters informed by data are those that move from their prior values—something that is straightforward to assess in the empirical analysis. The analysis presented in this figure is somewhat crude and is specific to the set of parameters sampled from the priors, which may or may not reflect real data. However, it gives a useful sense of the behaviour of the model inversion scheme in relation to this specific model (i.e. hypothesis) space.